MESOSCOPIC STRUCTURE OF PECTIN IN SOLUTION

Journal:	*Biopolymers*
Manuscript ID	BIP-2016-0181.R1
Wiley - Manuscript type:	Original Article
Date Submitted by the Author:	n/a
Complete List of Authors:	Alba, Katerina; University of Huddersfield, Biological Sciences Bingham, Richard; University of Huddersfield, Biological Sciences Kontogiorgos, Vassilis; University of Huddersfield, Biological Sciences
Keywords:	pectin, SAXS, polyelectrolyte, polysaccharide

MESOSCOPIC STRUCTURE OF PECTIN IN SOLUTION

K. Alba, R. J. Bingham, V. Kontogiorgos*

Department of Biological Sciences, University of Huddersfield, HD1 3DH, UK

*Corresponding author

Tel: 0044 -1484-472488.

e-mail address: v.kontogiorgos@hud.ac.uk

Abstract

Mesoscopic structure of pectin with different molecular characteristics was investigated by means of small angle X-ray scattering (SAXS), electrokinetic measurements and data modelling. The influence of a broad range of pH (2-7) on chain conformation in the dilute and semi-diluted regime was investigated. Scattering data and concomitant analysis revealed two length scales at all environmental conditions studied. pH showed greater influence at acidic values (pH 2.0) enhancing the globular component of the structure due to association of galacturonic acid residues. Double logarithmic scattering intensity plots revealed fractal dimensions of 1.9 ±0.2 in the low-*q* regime and 1.5 ±0.2 in the high *q*-region, irrespectively of the specific environment. Increase in branching of RG-I regions of the polysaccharide chains enhanced the compact conformation irrespectively of the pH or concentration. The present work shows that radical changes in pectin conformation can be induced only under strongly acidic conditions a finding that has important consequences in tailoring the technological performance of these biopolymers.

Keywords: pectin, SAXS, polyelectrolyte, polysaccharide

1. Introduction

The solution conformation of polysaccharides plays a determinant role in their functional properties. The first stage that is involved aqueous dispersion of biopolymers is hydration of the chains and exposure of the functional groups (e.g., hydroxyl, carboxyl, methyl, acetyl etc.). This is followed by interactions between the chains at the molecular level that lead to either self-association (i.e., aggregation) or heterotypic cooperation among different chains. The latter results in formation of three-dimensional structures (i.e., gels), biopolymer-biopolymer complexes or highly entangled viscous solutions. Mechanical properties and functional performance can be in most cases easily adjusted and the mechanistic underpinnings between the surrounding environment (e.g., pH, ionic strength, presence of cross linkers etc.) and chain behaviour are well understood.[1]

Pectin is a heteropolysaccharide of particular industrial importance (e.g., food and pharmaceutical industries) with diverse functionality due to its tunable primary structure. It is a diblock copolymer primarily consisting of homogalacturonan (HG) and rhamnogalacturonan I (RG-I) and the fine structure and functionalization of these two blocks control the properties of the biopolymer (Figure 1). Other moieties may be observed depending on the botanical origin and method of extraction such as rhamnogalacturonan II (RG-II), arabinogalactan, arabinan, apiogalacturonan and xylogalacturonan.[2] Proteins may also be attached to side chains of RG-I regions further contributing to the complexity of the structure (Figure 1). The presence of galacturonic acid residues (D-GalA) causes pectin to become negatively charged at neutral pH making it essentially an anionic polyelectrolyte. In addition, D-GalA residues are frequently methyl esterified yielding a range of pectins with different degree of methyl esterification. Typically, pectins with degree of methyl-esterification greater than 50% are described as high methyl-esterified (HM) and those with

lower than 50% are defined as low methyl-esterified (LM). *O*-Acetylation is also possible that usually occurs at the *O*-2 or *O*-3 position of rhamnose (Rha) or of D-GalA (Figure 1). The degree of methylation (DM) and acetylation (DA), in turn, may also influence conformational characteristics *via* hydrophobic interactions between chains.

This characteristic (i.e., free or methyl esterified D-GalA) makes solution conformation of pectin particularly responsive to the surroundings (e.g., ionic strength, pH, presence of divalent cations etc.) and to the fine structure (e.g., methyl and acetyl groups, molecular weight or branching). For that reason, the dispersion medium can be easily used to control functionality, as for instance in gelation or arrangement at the oil-water interface. As dispersion into an aqueous medium is always the first step towards a desired application, understanding of conformations and how they are affected by the various factors is key for tailoring pectin functionality. Previous small angle X-ray and neutron scattering and molecular modelling work on solution conformation of pectin has highlighted the importance of DM, rhamnose content, molecular weight [3] and HG/RG-I ratio [4] at neutral pH. However, interplay between the above parameters and pH, which control the functionality, has been largely disregarded. In the present investigation, therefore, we aim to unveil the relationships between concentration, branching and solvent pH on the solution conformation of pectin.

2. Materials and Methods

2.1 Materials

Pectin from okra pods with a low degree of methyl esterification was isolated and characterised as described elsewhere in detail.[5] Important chemical and physical characteristics relevant to the present investigation are reproduced in Table S1 in supplementary data. Samples were labelled as OP2 and OP6. Sodium chloride, citric and phosphate salts for buffer solutions (100 mM) were obtained from Sigma Aldrich (Poole, UK).

2.2 Sample preparation

Okra pectin was dispersed at 0.1 or 1.0 g dL^{-1} in 0.1 M buffers with pH 2.0, 4.0 (citric), 6.0 and 7.0 (phosphate) in the presence of 0.1 M NaCl. Samples were left overnight under continuous stirring to ensure complete solubilisation. Following solubilisation, samples were centrifuged to remove any insoluble cellulosic oligomers and were subjected to SAXS measurements at room temperature, as described in the next section.

2.3 SAXS measurements

SAXS data were acquired using a Bruker Nanostar from pectin solutions in the presence of 0.1 M NaCl. Samples of about 100 µl were sealed in a 1.5 mm bore quartz glass capillary and the sample chamber was evacuated to minimize background scattering. The sample to detector distance was 106.85 cm. The q-axis and beam centre were calibrated using the scattering pattern of silver-behenate salt (d-spacing = 5.84 nm). The momentum transfer was defined as $q = 4\pi\sin(\theta)/\lambda$ where θ is the scattering angle and λ the X-ray beam wavelength. Each scattering data set consisted of 5 × 5000 s exposures. Scattering data were collected at all pH values above and below the critical overlap concentration of the biopolymers (c*) that demarcates the dilute from semi-dilute regimes of the biopolymers. For each sample, the equivalent scattering data collected for buffer (5 × 5000 s) was subtracted using the Primus software.[6]

2.4. SAXS data analysis

Data analysis was performed using the software Scatter (v. 2.3H, BIOISIS). Cross sectional radius of gyration (R_c) was calculated using the Guinier approximation from the intermediate q-region so as $q \times R_c < 1.4$. Plots of $q^2 \times I(q)$ *versus* q (Kratky plots) were also constructed to examine the influence of pH on the conformation of the macromolecules. Double logarithmic intensity plots were also constructed and the fractal dimensions were

calculated from the exponents of power law regime of the curves. The exponents were calculated by fitting a power function of the form $f(x) = cx^{d_f}$ where c is a constant and d_f is the fractal dimension. The Ornstein-Zernike relationship was curve-fitted to the scattering intensity curves of semi-dilute solutions between 0.03 and 0.13 Å^{-1}. Non-linear regression of data (curve fitting) was performed using Prism v.6 (Graphpad Software, SanDiego, USA).

3. Results and Discussion

Figure 2 shows typical small-angle X-ray scattering intensity plots of pectin samples at all pH values in the presence of 0.1 M NaCl in the dilute (Fig 2a) and semi- dilute regime (Fig 2b) of the biopolymers. The screening from NaCl is required to prevent complexities that may stem from changes in chain dimensions due to intra- and inter- molecular electrostatic interactions.[7] In the presence of 0.1 M NaCl it is anticipated that the scattering curves reflect the conformations of the chains without intermolecular electrostatic interactions [7-10] and is a common practice in SAXS sample preparation of biological or synthetic polyelectrolytes. [3,11,12] It should be mentioned that it is possible to observe broadening of the scattering intensity curves at concentrations greater than the critical concentration (c*) of the biopolymers.[13] Nevertheless, the overall shape of the curves remains unaltered indicating negligible intermolecular interaction and no conformational changes at the concentrations studied. Additionally, NaCl provides adequate screening, as at low q no evident electrostatic peak is observed in the scattering patterns, something that is common in polyelectrolyte solutions in the absence of screening.[14,15] Although the shoulder at about 0.08 Å^{-1} could be related to the electrostatic peak or inter-backbone distances, electrostatic interactions do not show measurable influence on the structure and the intermolecular distance between pectin chains. As a result, the observed conformational changes can be comfortably attributed to the influence of solution pH. The peak at about 0.22 Å^{-1} (~ 29 Å)

could be related to side-chain interchain distance i.e., to the distance between the branches of RG-I units between different chains.

The scattering curves show marginal dependency on pH between 4 and 7 indicating that chain conformation is not particularly affected in this range. pH-Depended structures start developing by lowering pH below 4, an observation that is particularly evident in the semi dilute regime of the biopolymers (Fig 2b). It should be mentioned that scattering intensity increases for all samples in the semi dilute region because the number of scattering particles in the scattering volume increases with increasing concentration. ζ-Potential titration between pH 1.0 and 9.0 (Figure S1, supplementary data) reveal that below pH 4 there is a sharp decrease in biopolymer charge due protonation of the carboxyl groups of the galacturonic acid residues. At pH 2.0 biopolymer coils of both samples are almost devoid of charge (~ -4 mV) resulting in reduction in the strength of intramolecular interactions. The uniform decrease of the entire scattering intensity curve at pH 2.0 indicates that pH-dependent changes have been brought about in the pectin chains in the entire range of measured length scales. At limited electrostatic repulsions at pH 2, the compact conformations result in an overall reduction of total scattering intensity of both samples (Figure 2 and Figure 2b inset). This is expected, as scattering is proportional to the square of the particle volume and additional contributions may also be present from changes in scattering contrast.[16] It can be seen (Figure 2b *vs.* Figure 2b inset) that sample OP2 exhibits greater changes in scattering intensity with pH than OP6 demonstrating that acidic environments induce greater conformational modifications in this sample. OP6 higher scattering intensity is partially ascribed to the greater content of RG-I regions, as it will be discussed below in detail. Congruent results have been also reported for LM-pectin and chitosan solutions at different temperatures and concentrations. [17]

To further evaluate the influence of pH on the degree of disorder plots of $q^2I(q)$ *vs.* q (Kratky plots) were constructed (Figure 3). Curves show a distinct peak at about 0.07 $Å^{-1}$ followed by a sharp decay before starting increasing again at 0.15 $Å^{-1}$. Such a curve-shape is typical of partially folded chains with elongated domains corresponding to multidomain particles[18] indicating that pectin samples consist of regions with partially folded and extended conformations. This is also a common observation in multi-domain proteins, where flexible linkers connect two or more globular domains, resulting in Kratky plots with contributions from both of these structurally discrete regions.[19] Peaks at 0.07 $Å^{-1}$ have been previously observed for samples with multidomain structures[20] whereas the peak that occurs at about 0.21 $Å^{-1}$ has been attributed in cinerean solutions to the presence of rod-like structures.[21] The dual nature in the conformations of pectin particles seems to be preserved irrespectively of the pH values. It is difficult to assess quantitatively the extent to which pH affects conformations at this stage, however, qualitative inspection of Krakty plots show that peaks at 0.07 $Å^{-1}$, that indicate folded structures, become more prominent at low pH. These plots are recognizably different from Kratky plots that have been reported in the literature for λ-carrageenan and fucoidan in 0.5 M NaCl,[11] soy soluble polysaccharides,[22] carboxymethyl cellulose[23] or bacterial exo-polysaccharides[24] where chains adopt extended conformations without pronounced peaks. It appears that the prominence of neutral sugar RG-I branches in both samples (Table 1S, supplementary data), which is not influenced by changes in pH, serves as the basis for the compact conformation, as it is preserved at all pH values. This is in agreement with previous reports on the solution conformations of sugar beet pectin that revealed that fractions rich in RG-I regions are more compact than those rich in HG regions.[4,25] Additionally, the hydrophobic focal points of the chains (i.e., methyl and acetyl groups) should contribute to the folding of the chains *via* hydrophobic interactions. OP2 samples are overall more hydrophobic than OP6 but a clear link between hydrophobicity and

conformation cannot be distinguished at this stage. The multidomain character of the sample can be also visualised by observation of the pair distance distribution functions of the samples (Figure S2, supplementary data).

The Guinier approximation can be used to describe the scattering from samples that are asymmetric or elongated such that:

$$qI(q) \approx e^{-\frac{q^2 R_c^2}{2}} \qquad (1)$$

where R_c is the cross-sectional radius of gyration. Plots of $\ln(qI)$ *vs.* q^2 (Figure 2a, inset) yield the cross-sectional radius of gyration in the limit of $qR_c < 1.4$ (Table 1). All samples show a rise in the low q-values deviating from rod-like structures confirming that samples have several domains that is frequently observed in biological polyelectrolytes in solution. [11,26] On first inspection, all values of R_c (Table 1) range between 12-24 Å irrespectively of the pH of the solvent. Closer examination reveals that R_c has a tendency to decrease with the differences being more dramatic between pH 7.0 and pH 2.0. With decrease of pH the HG-pectin moieties fold as ionization of carboxyl groups decreases. On the contrary, high pH values result in extended conformations. At this pH, R_c is greater due to the exposure of the branched RG-I regions. This is indeed the case, as sample OP6 has larger R_c than OP2, as it has a greater molar ratio of RG-I regions although the higher molecular weight could also contribute (Table 1S, supplementary data). The R_c values are generally higher but comparable to other polysaccharides in solution reflecting the presence of bulky side chains. [11,26-28]

Double logarithmic plots of I(q) *vs.* q (Porod plots) can be used to provide information on the structural levels that are present in biopolymer coils and give a first insight to the conformation of the chains (Figure 4). Curves confirmed the two distinct length scales that are particularly evident in the samples above the c* of the coils (Figure 4b) with a transition occurring at 0.08 $Å^{-1}$. By fitting power law functions such as:

$$I(q) \sim I_0 q^{-d_f} \quad (3)$$

is possible to calculate the fractal dimensions of the coils from the exponent of equation 3 (Table 1). In the fractal regime the structure of the coils is independent of the length scale of observation and in real systems the self-similarity eventually terminates.[29] The two length-scales that are present in the biopolymers under investigation hold until about 0.08 $Å^{-1}$ and 0.2 $Å^{-1}$. Slope 1 fluctuates around -1.9 ±0.2 whereas slope 2 around -1.5 ±0.2 revealing scattering from mass fractal particles. A fractal dimension of 2 describes a random walk, while self-avoiding chains scale with exponent of 1.6. In terms of stiffness, random walk chains are more flexible than self-avoiding chains indicating that pectin contains rigid and flexible components in the structure. The first level of structure is related to the scattering of the entire chain and is associated with the length scale of R_g. A transition from power law with exponent -2 to -1.5 is related to the scattering of the second structural level which arises from local structural subunits[30] that for the present system should correspond to the length of the rod-like stiff structures. Mucins have shown similar behavior to the exponents with changes in pH[31] whereas apple pectin that lacks side chains and the complexity of the present samples has also revealed two length scales with slopes in the range of 2.1 and 1, for slopes 1 and 2, respectively.[32] Additionally, from the fractal exponents (Porod exponents) a first insight into the shape of the molecules can be also obtained. For instance, flat oblate ellipsoids have $d_f = 2$ whereas random coils in good solvent have $d_f = 5/3$ (1.6).[33] This is in agreement with atomic force microscopy imaging of pectin preparations where the macromolecular structures were described as "tadpoles" [34] containing two levels of distinct structures (i.e., globular plus linear). In that work, the role of protein (~8%) has been emphasized in the creation of these structures, which could also play a role to the structure formation of the samples in the present investigation (~5% protein, Table S1). Additionally, OP6 pectin shows marginally higher fractal dimensions than OP2, as a result of the more

extended branching of the chains (RG-I regions) that generally improve flexibility.[4] Variations in pH do not particularly affect the slopes indicating little change in the length scales of the macromolecules at all different conditions. The cross-sectional radius of gyration for rod-like structures can be converted into a length scale, that corresponds to the persistence length, l, of the constituent rods giving information about the stiffness of the chains. From theoretical point of view, ideal random coils have persistence lengths equal to zero whereas for extra-rigid rods it approaches infinity. In practice, the values range between 10-2000 Å for random coils (e.g. pullulan) or particularly rigid rods (e.g. DNA). [35,36] For polyelectrolytes, the total persistence length $l_{tot} = l_o + l_e$ is the sum of the persistence length of the chain in the absence (l_o) and presence (l_e) of electrostatic interactions. Since the latter interaction is screened by the high concentration of NaCl the chain dimensions will correspond to l_o. For these systems, an approximate l_o can be calculated through the R_c of a thin rigid rod, as $l = \sqrt{12R_c^2}$ and was found to be between 38-83 Å (3.8-8.3 nm) (Table 1), which is in close agreement with previously reported values (45-120 Å) indicating that pectin samples attain semi-flexible conformations.[3,4,25,36] In accordance with the R_c values, persistence length exhibits a step change between pH 7.0 and 2.0 due to folding of HG regions at acidic conditions showing remarkable decrease in stiffness from the neutral pH. It has been reported that increase in the RG-I domains leads to greater flexibility with persistence length values in the range between 20-30 Å.[4] Persistence length of OP6 samples, which are about 10% richer in RG-I domains than OP2 (Table 1S), are not in agreement with the above generalization probably due to differences in the molecular weight and D-GalA content. Finally, hydrophobicity (e.g., methyl and acetyl groups) is expected to play role in the flexibility on the chains. Previous studies reporting estimates of persistence length as a function of degree of methylation (DM) did not identify a clear relationship between DM and l_o. [3] In the present investigation, OP6 that is more hydrophobic displays a tendency to have

greater persistence lengths than OP2 at all pH values showing that it attains relatively stiffer conformations.

The scattering intensity from semi-dilute polymer solutions can be modeled using the Ornstein-Zernike relationship as:[37]

$$I(q) = \frac{I(0)}{1+q^2\xi^2} \quad (4)$$

where ξ is the correlation length of the chain and I(0) is the forward scattering intensity. At this juncture, it should be mentioned that for natural biopolymers is usually difficult to experimentally distinguish all three concentration regimes (i.e., dilute, semi-dilute (c*) and concentrated (c**)) as the demarcation lines between these regimes are usually blurred. Equation 4 usually describes well the scattering curves of biopolymer chains in homogeneous solutions but it fails in the case of solutions with inhomogeneities.[38] In the latter case, a second Debye–Bueche term[39] is needed to describe scattering that accounts for the correlations within the long-lived entanglements or aggregates. [40] By removing the Guinier regime [14] the second term in equation 4 is not required, thus we modelled the scattering from the semi-dilute regime fitting data from the power law region between ~0.03 and 0.13 $Å^{-1}$. The physical meaning of ξ, which is particularly affected by electrostatic interactions (e.g., pH, ionic strength),[7] is that at length scales smaller than ξ most of the monomers in the biopolymer chains are surrounded by the solvent or other monomers that belong to the same chain whereas at length scales greater than ξ chains entangle.[15] Estimates of correlation lengths at different pH values for both samples compare well with those of other polysaccharides (e.g., levan [40,41], carrageenan or methylcellulose [38]) and reveal an increase in ξ with pH for both samples due to electrostatic repulsion that increases the interaction distance of the chains.[27] In that case the size of the "mesh" that is formed by the overlapping chains increases resulting in a more open structure. Correlation length is greater for sample

OP6 than OP2 at all pH values. It is possible that the less extensive branching and lower molecular weight of OP2 gives the molecule the chance for more efficient packing thus decreasing the interaction distances. It emerges that a greater ξ value has consequences for the functional properties of pectin especially in relation to the interfacial arrangement. Combining information from our previous investigations [42,43] it seems that high ξ values correspond to weaker emulsion formation and stabilisation capacity of pectin. This observation is related to the thickness of the adsorbed interfacial layer [44] and the concomitant steric stabilisation.

4. Conclusions

The influence of pH on the solution conformation of pectin samples with distinct molecular characteristics and in the presence of 0.1 M NaCl was investigated using small angle X-ray scattering in the dilute and semi-dilute regime of the biopolymers. Irrespectively of the environmental conditions, pectin samples reveal two length scales that are maintained throughout the pH range that was employed (pH 2-7) corresponding to a mass fractal structure with d_f of about 2 and 1.5 for each length scale, respectively. At acidic pH (pH 2.0) a shift to more compact chain arrangements was observed whereas pH showed little influence at higher pH values (pH 4, 6, 7). Additionally, neutral sugar branches of RG-I moieties contribute to the creation of more compact conformations, irrespectively of the pH of the solvent.

5. References

1. Djabourov, M.; Nishinari, K.; Ross-Murphy, S. B. Physical Gels from Biological and Synthetic Polymers; Cambridge University Press: Cambridge, 2013.
2. Mohnen, D. Current Opinion in Plant Biology 2008, 11, 266-277.
3. Cros, S.; Garnier, C.; Axelos, M. A. V.; Imberty, A.; Perez, S. Biopolymers 1996, 39, 339-352.
4. Ralet, M.-C.; Crepeau, M.-J.; Lefebvre, J.; Mouille, G.; Hofte, H.; Thibault, J.-F. Biomacromolecules 2008, 9, 1454-1460.
5. Alba, K.; Laws, A. P.; Kontogiorgos, V. Food Hydrocoilloids 2015, 43, 726-735.
6. Konarev, P. V.; Volkov, V. V.; Sokolova, A. V.; Koch, M. H. J.; Svergun, D. I. Journal of Applied Crystallography 2003, 36, 1277-1282.
7. Dobrynin, A. V.; Colby, R. H.; Rubinstein, M. Macromolecules 1995, 28, 1859-1871.
8. Harding, E. S. Progress in Biophysics and Molecular Biology 1997, 68, 207-262.
9. Rinaudo, M. Structural Chemistry 2009, 20, 277-289.
10. Tomsic, M.; Rogac, M. B.; Jamnik, A. Acta Chimica Slovenica 2001, 48, 333-342.
11. Yuguchi, Y.; Tran, V. T. T.; Bui, L. M.; Takebe, S.; Suzuki, S.; Nakajima, N.; Kitamura, S.; Thanh, T. T. T. Carbohydrate Polymers 2016, 147, 69-78.
12. Nishida, K.; Kaji, K.; Kanaya, T.; Shibano, T. Macromolecules 2002, 35, 4084-4089.
13. Dror, Y.; Cohen, Y.; Yerushalmi-Rozen, R. Journal of Polymer Science Part B: Polymer Physics 2006, 44, 3265-3271.
14. Josef, E.; Bianco-Peled, H. Soft Matter 2012, 8, 9156-9165.
15. Salamon, K.; Aumiler, D.; Pabst, G.; Vuletic, T. Macromolecules 2013, 46, 1107-1118.
16. Svergun, D. I.; Koch, M. H. J.; Timmins, P. A.; May, R. P. Small Angle X-Ray and Neutron Scattering from Solutions of Biological Macromolecules; Oxford University Press: Oxford, 2013.
17. Ventura, I.; Bianco-Peled, H. Carbohydrate Polymers 2015, 123, 122-129.
18. Rambo, R. P.; Tainer, J. A. Biopolymers 2011, 95, 559-571.
19. Bernado, P.; Svergun, D. I. Molecular BioSystems 2012, 8, 151-167.
20. Qazvini, N. T.; Bolisetty, S.; Adamcik, J.; Mezzenga, R. Biomacromolecules 2012, 13, 2136-2147.
21. Gawronski, M.; Conrad, H.; Stahmann, K. P. Macromolecules 1996, 29, 7820-7825.
22. Chivero, P.; Gohtani, S.; Ikeda, S.; Nakamura, A. Food Hydrocolloids 2014, 35, 279-286.
23. Dogsa, I.; Tomsic, M.; Orehek, J.; Benigar, E.; Jamnik, A.; Stopar, D. Carbohydrate Polymers 2014, 111, 492-504.
24. Dogsa, I.; Kriechbaum, M.; Stopar, D.; Laggner, P. Biophysical Journal 2005, 89, 2711-2720.
25. Morris, G. A.; Ralet, M.-C. Carbohydrate Polymers 2012, 88, 1488-1491.
26. Stokke, B. T.; Draget, K. I.; Smidsrød, O.; Yuguchi, Y.; Urakawa, H.; Kajiwara, K. Macromolecules 2000, 33, 1853-1863.
27. Yuguchi, Y.; Mimura, M.; Urakawa, H.; Kitamura, S.; Ohno, S.; Kajiwara, K. Carbohydrate Polymers 1996, 30, 83-93.
28. Muller, F.; Manet, S.; Jean, B.; Chambat, G.; Boue, F.; Heux, L.; Cousin, F. Biomacromolecules 2011, 12, 3330-3336.
29. Teixeira, J. Journal of Applied Crystallography 1988, 21, 781-785.
30. Beaucage, G. Journal of Applied Crystallography 1996, 29, 134-146.

31. Georgiades, P.; di Cola, E.; Heenan, R. K.; Pudney, P. D. A.; Thornton, D. J.; Waigh, T. A. Biopolymers 2014, 101, 1154-1164.
32. Mansel, B. W.; Chu, C.-Y.; Leis, A.; Hemar, Y.; Chen, H.-L.; Lundin, L.; Williams, M. A. K. Biomacromolecules 2015, 16, 3209-3216.
33. Putnam, C. D.; Hammel, M.; Hura, G. L.; Tainer, J. A. Quarterly Reviews of Biophysics 2007, 40, 191-285.
34. Kirby, A. R.; MacDougall, A. J.; Morris, V. J. Carbohydrate Polymers 2008, 71, 640-647.
35. Tombs, M. P.; Harding, S. E. An introduction to polysaccharide biotechnology; Taylor and Francis: London, 1998.
36. Morris, G. A.; de al Torre, J. G.; Ortega, A.; Castile, J.; Smith, A.; Harding, S. E. Food Hydrocolloids 2008, 22, 1435-1442.
37. Yukioka, S.; Higo, Y.; Noda, I.; Nagasawa, M. Polym J 1986, 18, 941-946.
38. Cerar, J.; Jamnik, A.; Tomšič, M. Acta Chimica Slovenica 2015, 62.
39. Debye, P.; Bueche, A. M. Journal of Applied Physics 1949, 20, 518-525.
40. Benigar, E.; Dogsa, I.; Stopar, D.; Jamnik, A.; Cigić, I. K.; Tomšič, M. Langmuir 2014, 30, 4172-4182.
41. Benigar, E.; Zupančič Valant, A.; Dogsa, I.; Sretenovic, S.; Stopar, D.; Jamnik, A.; Tomšič, M. Langmuir 2016, 32, 8182-8194.
42. Alba, K.; Sagis, L. M. C.; Kontogiorgos, V. Colloids and Surfaces B: Biointerfaces 2016, 145, 301-308.
43. Alba, K.; Kontogiorgos, V. Food Hydrocolloids 2016, doi: 10.1016/j.foodhyd.2016.1007.1026.
44. Dobrynin, A. V.; Rubinstein, M. Progress in Polymer Science 2005, 30, 1049-1118.

FIGURE LEGENDS

Figure 1: Schematic representation of major pectin building blocks primarily responsible for conformational characteristics of pectin in solution. HG is the homogalacturonan and RG-I is the rhamnogalacturonan-I regions.

Figure 2: Small-angle X-ray scattering intensity plots of OP2 pectin samples at all pH values in the presence of 0.1 M NaCl in the (a) dilute and (b) semi-dilute regime of the biopolymer. Top right inset shows how the cross-sectional radius of gyration was calculated from ln(I) *vs.* q^2 plots. Bottom right inset shows scattering intensity plots of sample OP6 at the semi-dilute regime.

Figure 3: Kratky plots of samples of OP2 samples in the (a) dilute and (b) semi-dilute regime of the biopolymers. A peak at about 0.07 $Å^{-1}$ followed by a sharp decay before starting increasing again at 0.15 $Å^{-1}$ indicates partially folded chains with elongated domains corresponding to multi-domain particles.

Figure 4: Porod plots of (a) OP6 in the dilute and (b) OP2 in the semi-dilute regime of the biopolymers with a transition occurring at 0.08 $Å^{-1}$. Slopes are also shown for each region.

Table 1: Molecular characteristics of samples obtained from SAXS data analysis.

		R_c (Å)	Slope 1	Slope 2	l_o (Å)	ξ (Å)[a]
OP2 Dilute	**pH 2**	12	-1.8	-1.0	42	-
	pH 4	15	-1.9	-1.5	52	-
	pH 6	15	-2.0	-1.3	52	-
	pH 7	20	-1.5	-1.4	69	-
OP2 Semi dilute	**pH 2**	15	-1.8	-1.4	52	32 (0.962)
	pH 4	16	-1.9	-1.8	55	50 (0.950)
	pH 6	16	-1.9	-1.8	55	55 (0.932)
	pH 7	21	-2.0	-1.8	73	97 (0.876)
OP6 Dilute	**pH 2**	11	-2.1	-1.0	38	-
	pH 4	17	-2.0	-1.5	59	-
	pH 6	20	-2.0	-1.5	69	-
	pH 7	24	-1.5	-1.6	83	-
OP6 Semi dilute	**pH 2**	19	-2.3	-1.5	66	65 (0.925)
	pH 4	20	-2.1	-1.7	69	102 (0.960)
	pH 6	21	-2.2	-1.8	73	106 (0.904)
	pH 7	23	-2.1	-1.8	80	154 (0.824)

a: Value in the brackets shows the r^2 of fitting the Ornstein-Zernike relationship to the SAXS data

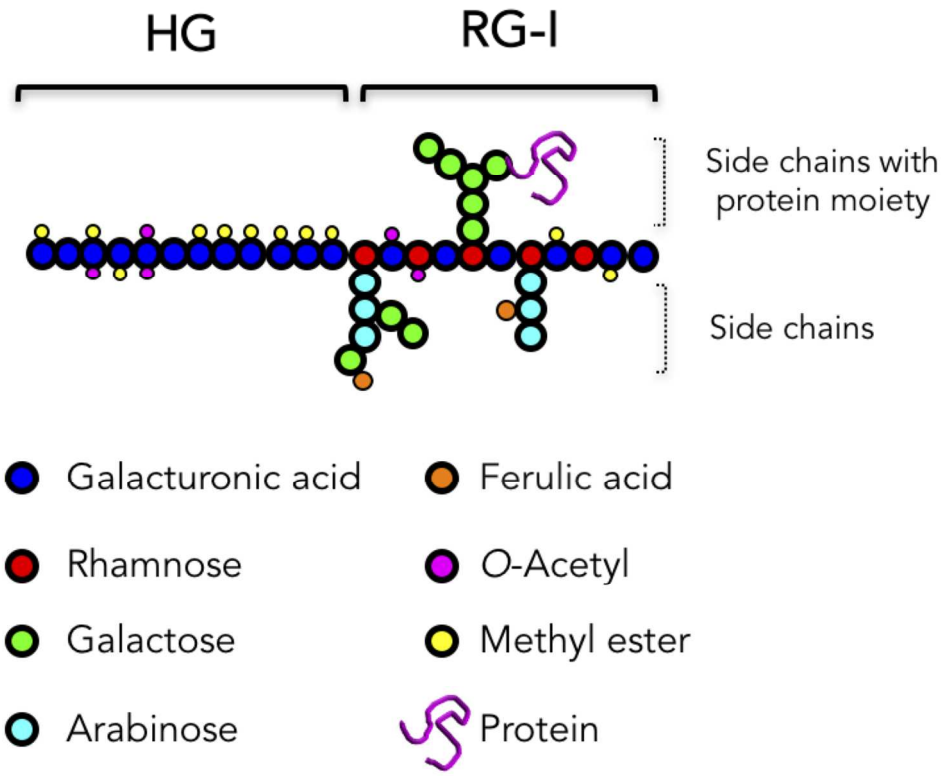

Schematic representation of major pectin building blocks primarily responsible for conformational characteristics of pectin in solution. HG is the homogalacturonan and RG-I is the rhamnogalacturonan-I regions.

128x105mm (300 x 300 DPI)

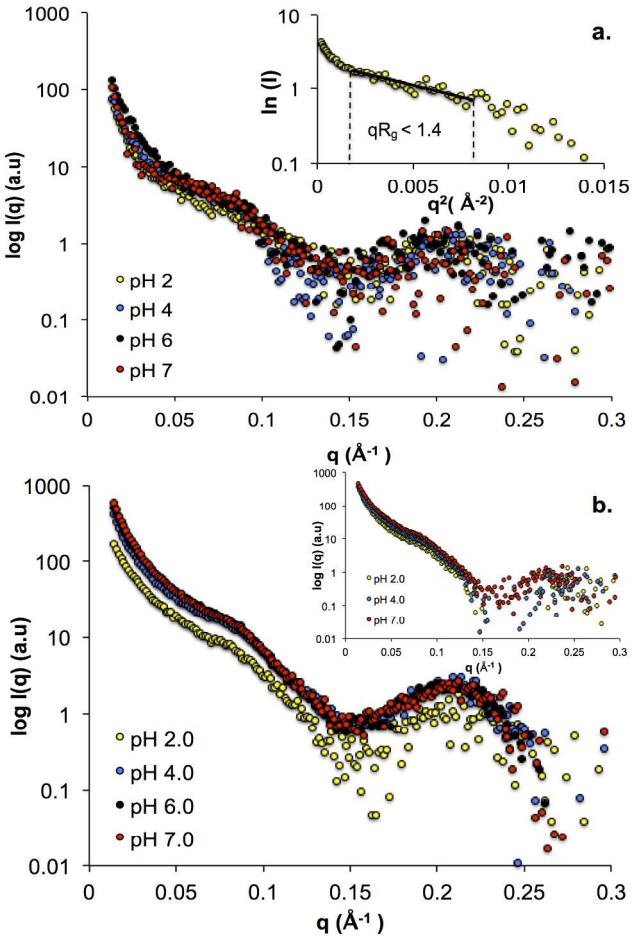

Small-angle X-ray scattering intensity plots of OP2 pectin samples at all pH values in the presence of 0.1 M NaCl in the (a) dilute and (b) semi-dilute regime of the biopolymer. Top right inset shows how the cross-sectional radius of gyration was calculated from ln(I) vs. q2 plots. Bottom right inset shows scattering intensity plots of sample OP6 at the semi-dilute regime.

215x279mm (300 x 300 DPI)

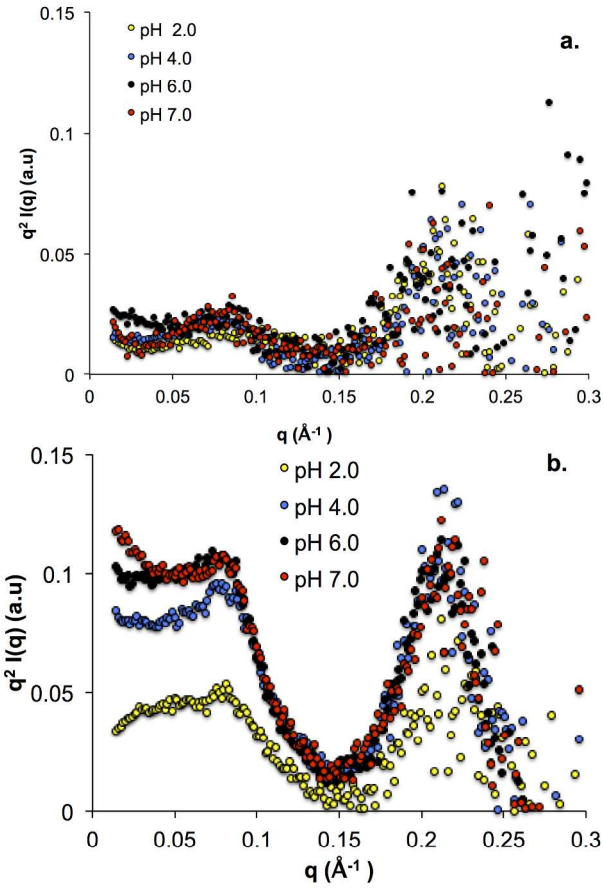

Kratky plots of samples of OP2 samples in the (a) dilute and (b) semi-dilute regime of the biopolymers. A peak at about 0.07 Å-1 followed by a sharp decay before starting increasing again at 0.15 Å-1 indicates partially folded chains with elongated domains corresponding to multi-domain particles.

215x279mm (300 x 300 DPI)

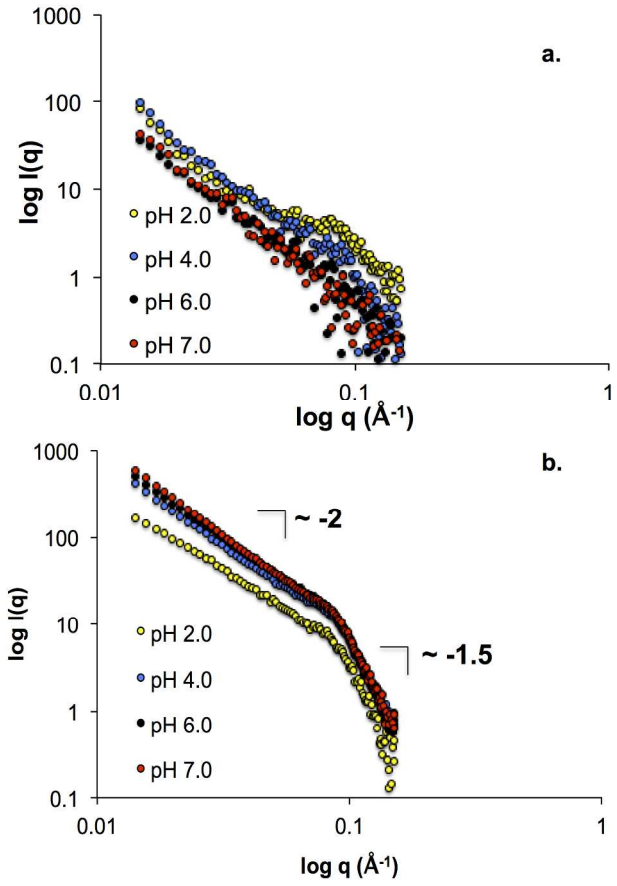

Porod plots of (a) OP6 in the dilute and (b) OP2 in the semi-dilute regime of the biopolymers with a transition occurring at 0.08 Å-1. Slopes are also shown for each region.

215x279mm (300 x 300 DPI)